6th International Supercritical Power Cycles Symposium
March 27-29, 2018, Pittsburgh, Pennsylvania

Managing Thermal Gradients on a Supercritical CO_2 Radial Inflow Turbine

David W. Stevens
Peregrine Turbine Technologies
dstevens@peregrineturbine.com

David W. Stevens, Lead Analysis Engineer

David holds a BSME from the University of Southern Maine and functions as a multi-disciplinary analyst at Peregrine Turbine Technologies. Analysis specialties include thermal, rotordynamics, and structures. David utilizes his strong analytical skills to solve difficult design challenges in rotating and static components. David's recent work includes thermal and rotordynamics analysis performed for the Air Force Research Lab and Office of Naval Research under a SBIR Phase III contract. Prior to his engineering education, David was an accomplished mechanical and electrical technician in the marine industry. David utilizes these skills at Peregrine in testing, prototyping, and product support.

Abstract

Historically, a consistent engineering challenge in the design of rotor and blade elements in turbine hot sections is sufficiently cooling the turbine rotor and blade structures to assure machine durability. Turbine inlet temperatures are often above the melting point of the metals employed in these parts. Sophisticated cooling strategies have been employed for many decades in order to make this possible. The use of supercritical carbon dioxide (sCO_2) as a thermodynamic working fluid presents somewhat of a different problem. Turbine inlet temperatures for these systems are generally limited by the capabilities of the primary heat exchanger rather than the turbine itself. For that reason, the author has not seen designs proposed for turbine inlet temperatures above 750°C (1382°F). At this lower inlet temperature, sophisticated cooling passages within rotating structures is not required. In fact, this is considered a low temperature even for turbochargers.

Instead, the challenge to utilizing sCO_2 originates from its thermo-physical heat transfer properties and particularly their effects on turbine back face cooling. The Peregrine Turbine Technologies (PTT) 1MW turbo pump features a single radial inflow high pressure turbine (HPT). A Steady state and transient rotor stator heat transfer analysis was performed on the 1MW turbo pump. Results of the analysis revealed an engineering challenge contrary to traditional air cooled radial turbine wheels. Temperature plots of the 1MW HPT showed strong thermal gradients on the back face caused by overcooling. Resulting stress model results revealed thermally induced stresses in the HPT above fatigue design criteria. A unique

secondary flow cooling method was utilized to reduce the stress to an acceptable level. This paper will examine the root of the problem and present a successful solution.

Introduction

Turbomachinery engineers routinely utilize secondary flows to cool high temperature rotating turbomachinery components such as blades and disks in air breathing engines. This is accomplished by routing fractions of compressor discharge through specialized cooling holes in blades or up the back face of a bladed disk. Utilizing compressor discharge flow for cooling purposes results in a system performance loss. However, this loss allows the machine to operate at a higher turbine inlet temperature and results in increased thermal efficiency. Current sophisticated cooling technologies permit turbine inlet temperatures in excess of 1600°C in gas turbine engines. Current reciprocating engine turbocharger technologies allow for turbine inlet temperatures above 1000°C. Nonetheless, current sCO_2 turbines are limited to inlet temperatures of 750°C. This limitation is a consequence of primary heat exchanger temperature limitations. The PTT 1MW turbopump HPT is currently aligned with this temperature.

sCO_2 features unique properties that are conducive for use as a turbomachinery power cycle working fluid. One feature is thermo-physical properties which greatly enhance convective heat transfer. This feature is very advantageous in heat exchanger applications. However, when utilized to cool the back face of a bladed disk, this enhancement can result in excessive convective heat transfer and large thermal gradients. This fact was revealed in the results of a steady state and transient rotor stator heat transfer finite element analysis (FEA) of the PTT 1 MW turbopump HPT. Subsequent structural FEA models revealed very high thermally induced stresses beyond acceptable fatigue design criteria.

A detailed examination of the problem and the solution are contained in the following paragraphs. First, a better understanding of the problem is accomplished via an examination and discussion of how thermo-physical properties directly impact convective heat transfer coefficients. This includes a comparison of air and sCO_2 at typical gas turbine operating temperatures and pressures. Second, the successful secondary flow solution utilized is described. Third, a brief overview of the thermal and structural FEA models utilized to identify and solve the problem are presented. Lastly, thermal and structural model results before and after solution implementation are presented in the form of isothermal and stress plots.

Thermo-physical Properties of sCO_2

The root of the thermal gradient problem is the high heat transfer coefficients produced by the unique thermo-physical properties of sCO_2. As previously mentioned, hot section parts in air breathing machines are effectively cooled using secondary flows. Moreover, the author is unaware of a similar problem occurring in an air breathing engine. Therefore, valuable understanding of the thermal gradient problem in the HPT is accomplished by examining how thermo-physical properties effect basic convective heat transfer in sCO_2 vs. air. This is performed by examining how the properties effect fundamental convective heat transfer equations and dimensionless quantities.

Convective heat transfer is governed by fluid thermo-physical properties, fluid velocity v, and geometry of the solid surface. Thermo-physical properties include dynamic viscosity μ, thermal conductivity k, density ρ, and specific heat c_p. Geometric properties of the solid surface include the friction factor f, and

characteristic length L_c. The previous properties and quantities determine the dimensionless parameters Reynolds Number Re (Eq.1), Prandtl Number Pr (Eq.2) and Nusselt Number Nu (Eq.3). The computation of an appropriate Nusselt correlation determines the surface heat transfer coefficient h. The specific rotor stator Nusselt correlations utilized for the thermal analysis performed are beyond the scope of this document. However, The Chilton-Colburn correlation (Eq.3) will be utilized throughout this document as a base to compare resulting Nusselt numbers and heat transfer coefficients.

Equation 1.
$$\boldsymbol{Re = \frac{Inertial\ forces}{Viscous\ forces} = \frac{\rho v L_c}{\mu}}$$

Equation 2.
$$\boldsymbol{Pr = \frac{Molecular\ diffusivity\ of\ momentum}{Molecular\ diffusivity\ of\ heat} = \frac{\mu c_p}{k}}$$

Equation 3.
$$\boldsymbol{Nu = \frac{hL_c}{k} = 0.023 Re^{0.8} Pr^{1/3}\ for\ \begin{Bmatrix} 0.5 \le Pr \le 160 \\ Re \ge 10^4 \end{Bmatrix}}$$

sCO_2 turbopumps and air gas turbines operate at very different temperatures and pressures. Therefore, a comparison between sCO_2 and air is best performed at the temperatures and pressures typical to each type of machine. Most sCO_2 machines operate at pressures from 1000 - 7000 psi, and temperatures between 100 - 1382°F (750°C). On the other hand, air gas turbines typically operate at pressures from ambient to 400 psi and temperatures between ambient and 2900°F (1600°C). As stated previously, compressor discharge gas is typically utilized to cool hot turbine components. Compressor discharge pressures and temperatures (P_2, T_2) for an air gas turbine can reach (400 psi, 1000°F) while the discharge for the 1MW turbopump is (6220 psi, 190°F). Isobaric thermo-physical properties of air and sCO_2 are compared in Figures 1-4. Isobaric dimensionless parameters are compared in figures 5-7. Isobar ranges for sCO_2 and air are in accordance with the previously mentioned typical operating pressures and temperatures. All isobars were computed using CoolProp[1].

A major difference between the properties of air and sCO_2 are apparent upon first inspection of Figures 1-5. The distance between the sCO_2 isobars vary greatly as temperature decreases. The distance between isobars for air also increases at lower temperatures. However, the distances are small, uniform, and quickly converge to near unity as temperature increases. The increase in differences as temperature decreases is due to the 87.98°F critical temperature of sCO_2. That is, as the gas approaches critical pressure and temperature (1071 psi, 87.98°F) the thermo-physical properties will vary greatly. This difference reveals the necessity to observe real gas properties and utilize proper equations of state such as Span and Wagner 1996 when performing heat transfer and fluids analysis of sCO_2.

The dimensionless parameters Reynolds number Re, Prandtl number Pr, and Nusselt Number Nu are functions of the thermo-physical properties (k, c_p, μ, ρ). Thus, an examination of their differences is required first.

Thermal conductivity k is equal to the molecular diffusivity of heat. More specifically, higher thermal conductivity indicates lower resistance to heat flow through a media. As shown in figure 1, thermal conductivity of sCO_2 ranges between 0.015 – 0.075 Btu/hr-ft-°F near the critical temperature. At the upper end of the domain, the range narrows to 0.041 – 0.05 Btu/hr-ft-°F. The different isobars for air are not discernable and range almost linearly between 0.015 – 0.063 Btu/hr-ft-°F across the domain. At the

[1] (CoolProp, 2016)

previously defined compressor discharge conditions the thermal conductivity of sCO_2 is over 1.5x greater than air. The increased thermal conductivity in sCO_2 will enhance the convective heat transfer.

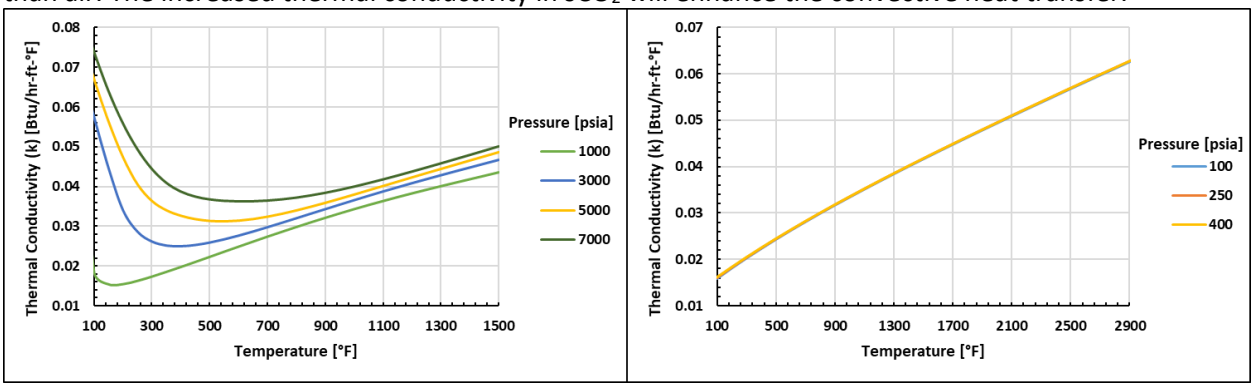

Figure 1. Thermal conductivity isobars vs. temperature (sCO_2 left, air right)

Specific heat c_p describes the amount energy required to raise the temperature of given mass by a explicit amount. In other words, the thermal capacity of a substance. As shown in figure 2, thermal conductivity of sCO_2 near the critical temperature ranges between 0.26-0.69 Btu/lbm-°F. At the upper end of the domain, the range converges to approximately 0.31 Btu/lbm-°F. However, air only ranges between 0.24 – 0.29 across the entire temperature domain. At the previously defined compressor discharge conditions the specific heat of sCO_2 is almost 2x greater than air. The increased specific heat in sCO_2 will enhance the convective heat transfer because the fluid is able to transport more heat energy.

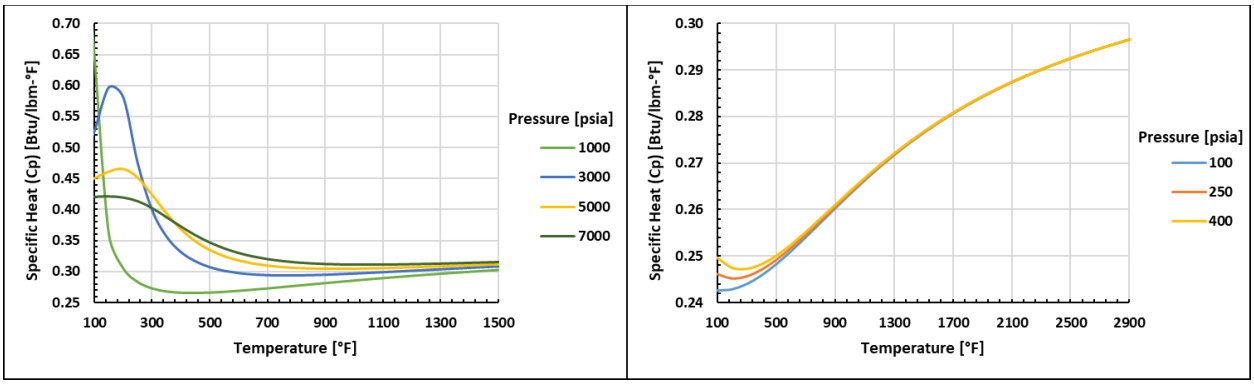

Figure 2. Specific heat isobars vs. temperature (sCO_2 left, air right)

Dynamic viscosity μ describes the resistance to shear flow. As shown in figure 3, the dynamic viscosity of sCO_2 near the critical temperature ranges between $1.0x10^{-5}$ – $8.0x10^{-5}$ lbm/ft-s. At the upper end of the domain, the range converges to approximately $3x10^{-5}$ lbm/ft-s. The different isobars for air are not discernable and range almost linearly between $1.0x10^{-5}$ – $4.5x10^{-5}$ lbm/ft-s across the domain. At the previously defined compressor discharge conditions the dynamic viscosity of sCO_2 is 2x greater than air. Based on equations 2 and 3 a larger dynamic viscosity will result in lower Reynolds numbers and larger Prandtl numbers.

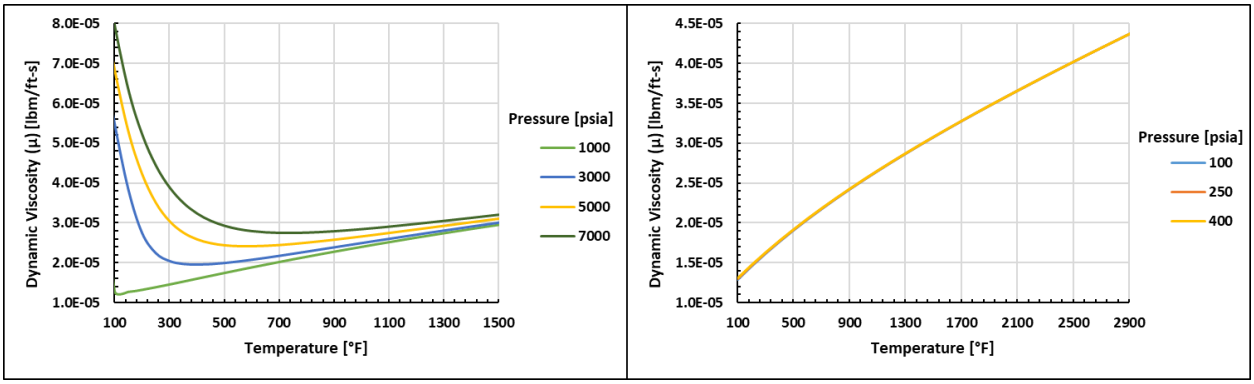

Figure 3. Dynamic viscosity isobars vs. temperature (sCO_2 left, air right)

Density ρ describes the mass per unit volume of a substance. As shown in figure 4, sCO_2 is a much denser fluid than air. Moreover, both fluids are compressible. At the previously defined compressor discharge conditions the density of sCO_2 is 70x greater than air. The dramatically higher density sCO_2 results in much higher inertial forces in the flow. This results in larger Reynolds numbers in accordance with equation 1.

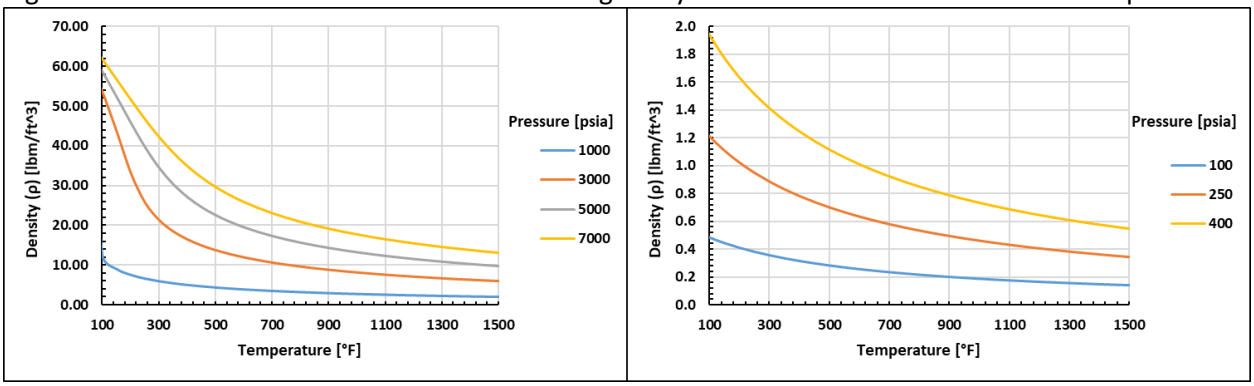

Figure 4. Density isobars vs. temperature (sCO_2 left, air right)

Prandtl number (Eq.2) (Fig.5) describes the ratio of the rate at which momentum and heat dissipate through a fluid. The molecular diffusivity of momentum is equal to the product of the dynamic viscosity μ (Fig.4), and specific heat c_p (Fig.3). The molecular diffusivity of heat is equal to the thermal conductivity k (Fig.2).

A Prandtl number of 1 indicates momentum and heat dissipate through the fluid at equal rates. As shown in figure 5, the Prandtl number of sCO_2 near the critical temperature ranges between 0.72 – 1.44. At the upper end of the domain, the range converges to approximately 0.7. However, air only ranges between 0.7 and 0.75 across the entire domain. At the previously described typical compressor discharge conditions the Prandtl number of the air will be approximately 0.72, and 1.44 for sCO_2. The Prandtl number of the sCO_2 is 2x that of the air. in most cases, for an sCO_2 machine, the thermal boundary layer will be thinner relative to the velocity boundary layer. The inverse will be true for an air machine. The thinner thermal boundary layer in the sCO_2 machine will enhance convective heat transfer.

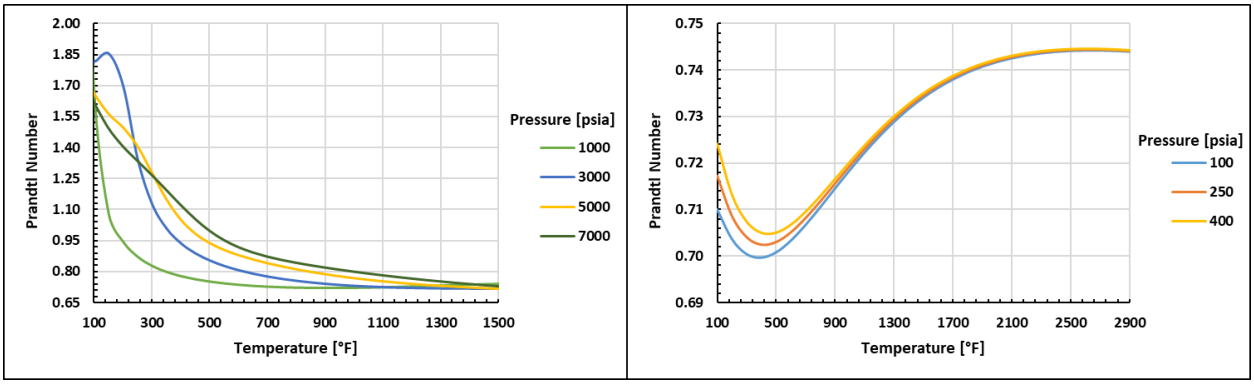

Figure 5. Prandtl Number isobars vs. temperature (sCO_2 left, air right)

Reynolds number (Eq.1) describes the ratio of the inertial forces to the viscous forces in the fluid flow. This is equal to the product of the density ρ (Fig.4), velocity v, and characteristic length L_c divided by the dynamic viscosity μ (Fig.3). Because the Reynolds number is a function of (v, L_c) an assumption must be made to compare isobars of sCO_2 and air. If velocity v and characteristic length L_c are assumed to be constant and equal to 1 the Reynolds number becomes a non-dimensional ratio of the magnitude of ρ/μ. The results shown in figure 6 depict sCO_2 Reynolds number isobars an order of magnitude larger than air at the defined range of pressures and temperatures for each machine type respectively. At the previously defined compressor discharge conditions the Reynolds number of the sCO_2 is 35x greater than air. These results agree with the previous examinations of density ρ and dynamic viscosity μ. This results in larger Reynolds numbers in accordance with equation 1. The dramatically higher Reynolds numbers will result in much higher heat transfer coefficients due to the increased turbulence of the flow.

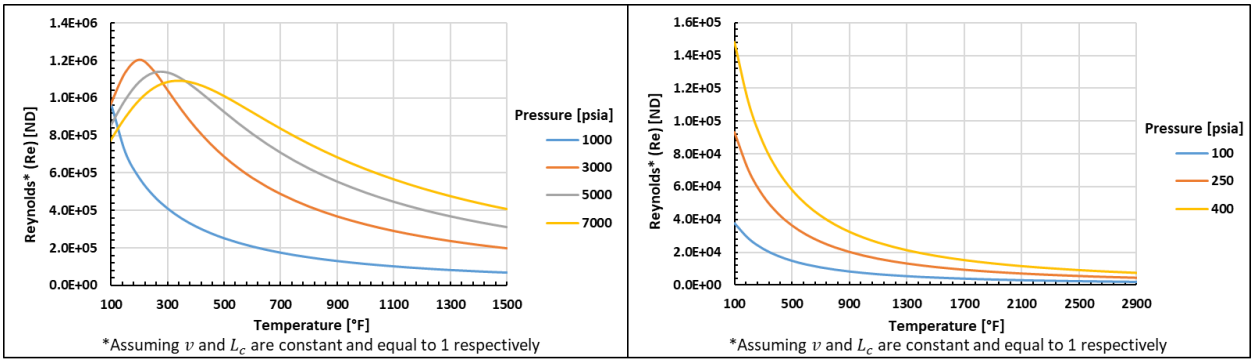

Figure 6. Reynolds number isobars vs. temperature (sCO_2 left, air right)

The Nusselt number describes the magnitude of convection on a surface. In other words, the higher the Nusselt number, the more the heat transfer is dominated by convection rather than conduction. Nusselt correlations allow the computation of Nusselt number based on empirical data. As stated previously, the Nusselt number can then be utilized to determine a heat transfer coefficient h. Most Nusselt correlations are functions of Prandtl and Reynolds numbers raised to a power between 0 and 1. The example used here is the Chilton-Colburn equation defined in equation 3. Other, more complex correlations also utilize other variables such as friction factor f. Extending the assumption utilized in the computation of Reynolds number isobars, Chilton-Colburn equation Nusselt number isobars are computed. The results shown in figure 7 depict sCO_2 Nusselt number isobars an order of magnitude larger than air at the defined range of pressures and temperatures for each machine type respectively. At the previously defined compressor discharge conditions the Nusselt number of the sCO_2 is almost 22x greater than air.

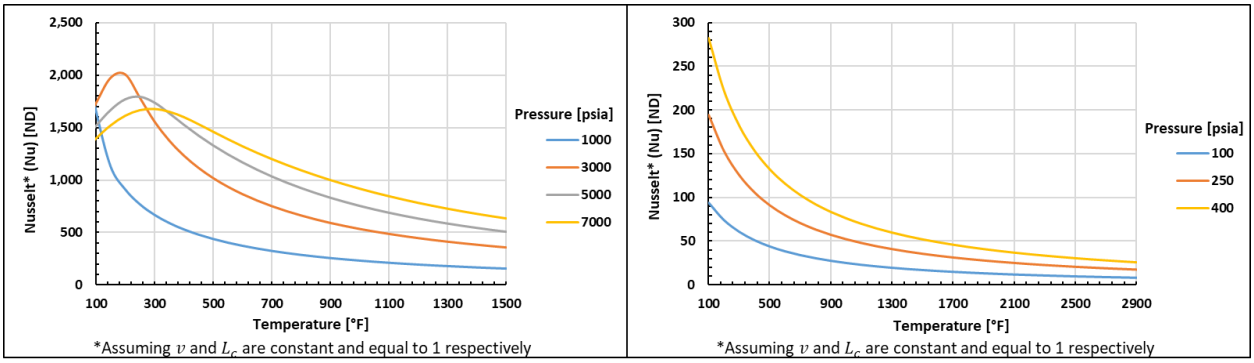

Figure 7. Nusselt number isobars vs. temperature (sCO_2 left, air right)

These drastically higher Nusselt numbers indicate high, convection dominated heat transfer coefficients h. Consequently, high heat flux $\dot{Q}$ will result and tend to drive the solid surface temperature T_s closer to the mean fluid temperature T_m. The Nusselt numbers calculated for the HPT back face and primary flow surfaces at the SS max condition were of the same order of magnitude (10^3) as depicted in Figure 7. (left). Results of the 1MW turbo pump thermal model depict a thermal tug-of-war between the heating of the HPT primary flow surfaces and cooling of the back face. The high h values inherent to the sCO_2 fluid cause the primary surfaces and back face of the HPT to be driven close to the mean temperature T_m of the respective flow. In the case of the 1MW HPT at SS max where $T_3 = 1382°F$ and $T_2 = 190°F$ (cooling supply temperature) the result is a steep thermal gradient through the bladed disk. Indeed, transient conditions will intensify this problem. Detailed results and discussion are contained in the results section.

Mitigation

Changes to geometry and secondary flows were utilized to mitigate the thermal gradients and peak stresses in the HPT. Changes to geometry were employed first but were unable to sufficiently reduce the peak stresses to an acceptable level to meet fatigue limits of the material. As described in the thermo-physical fluid properties discussion, the root cause of the problem is aggressive convective cooling of the HPT back face. Therefore, the practical solution was modification of the secondary flow regime. The most obvious solution was a reduction of mass flow on the HPT back face. However, the overall mass flow rate was already very low. Moreover, the flow could not be eliminated because the aft radial bearing is cooled by flow upstream of the HPT back face. Complete elimination of the cooling flow would allow hot gas ingestion from the HPT inlet into the bearing.

A less obvious approach was required to solve the problem. Instead, the cooling flow could be preheated to increase the temperature of the HPT back face. The result would reduce the thermal gradient on the HPT back face. This could be accomplished by recirculating a fraction of the cooling flow downstream of the HPT back face rather than injecting the entire flow into the HPT inlet. However, this solution was not without risk. The preheating recirculation loop could add too much heat to the flow and the bearing upstream of the HPT back face could overheat.

The secondary flow and FEA thermal model was modified to test this approach. Dramatic increases in HPT back face temperature and decreases in the thermal gradient resulted. Moreover, results showed ample cooling of the aft radial bearing. Subsequent structural analysis results showed large decreases in peak stresses. Figure 10 details the preheating recirculation loop concept. Detailed thermal and structural FEA model results are discussed in the next section.

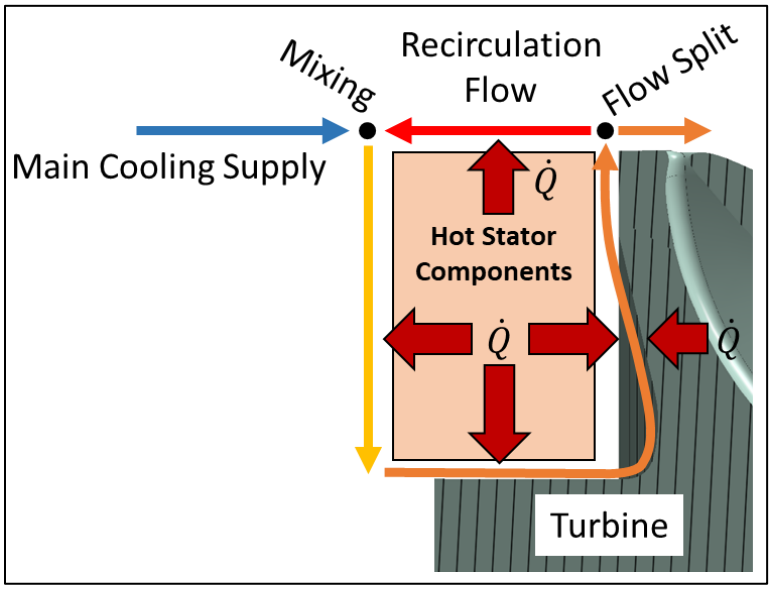

Figure 10. HPT cooling flow recirculation/preheating

Finite Element Models

The PTT 1MW turbopump rotor stator thermal model was constructed and solved using ANSYS APDL. Solid bodies were modeled using ten node tetrahedral elements. A thermal fluid convection network of primary and secondary flows was modeled using FLUID116 elements. Model inputs were comprised of aerodynamic analysis outputs, and secondary flow analysis outputs. A single model was utilized to obtain steady state and transient results. Figure 8 shows the solid body mesh of the HPT. Figure 9 illustrates HPT back face portion of the thermal fluid network.

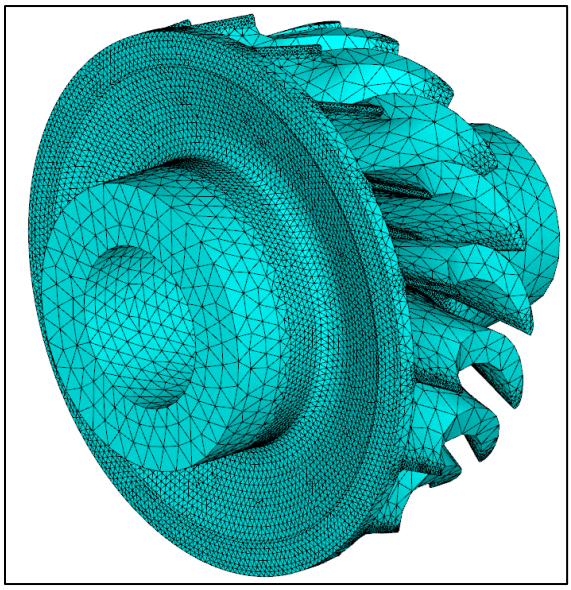

Figure 8. HPT solid body thermal mesh

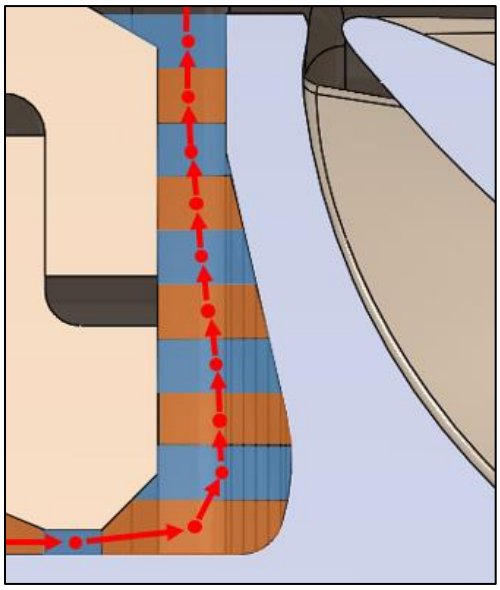

Figure 9. HPT back face fluid network

The structural rotor model was constructed and solved using ANSYS Mechanical. Solid bodies were meshed using ten node tetrahedral elements. Temperature results from the thermal model were applied to the solid bodies via triangulation in ANSYS. Angular velocity, surface pressures, and assembly loads were also applied to the model.

Results and Discussion

The high heat transfer coefficients inherent to sCO_2 coupled with the large temperature differences between the back face cooling and HPT inlet flows are the driver of the large thermal gradients in the HPT. Hence, the maximum thermal gradient in the HPT occurs when the temperature difference between the two flows is largest. Therefore, transient effects can greatly intensify the thermal gradient. For example, if the HPT inlet temperature increases faster than the cooling flow temperature during a burst or decreases similarly during a chop. A 16 second idle to max burst and max to idle chop time was utilized in the 1MW turbo pump thermal analysis. With the preheating loop implemented, this ramp rate produced peak thermal gradients at 2 seconds post burst, and 4 seconds into chop. Despite the aggressive ramp rate, the peak thermal gradients and resulting stresses were less than 5% higher than at SS max. A transient analysis without the recirculation loop has yet to be performed by the author. Therefore, only SS max results before and after implementation of the preheating loop are shown and discussed below. Thermal and stress model results are presented in figures 11-15.

Figure 11 displays isothermal solid body temperatures before and after the implementation of the preheating loop. Preheating the flow by recirculation increases the minimum HPT body temperature at the hub by more than 100°F.

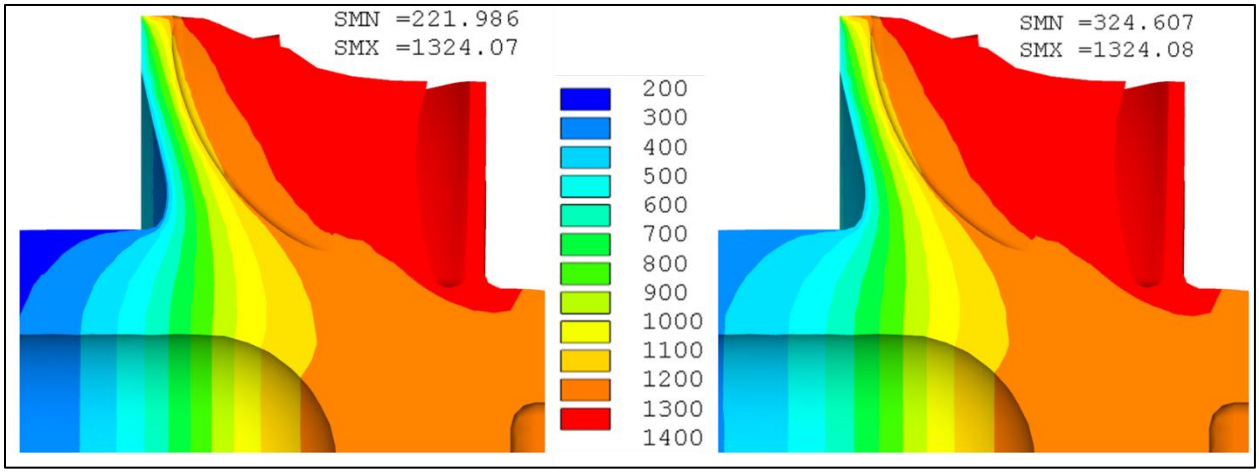

Figure 11. SS max HPT isothermal Plot (°F). No recirculation flow left. With recirculation flow right. (SMN and SMX are maximum and minimum temperatures)

Figures 12-13 display before and after mean fluid T_m and surface T_s temperatures. Note the 87°F increase in T_m at the hub after implementation of the preheating loop. Additionally, all surface temperatures T_s are between 10-20% different than the adjacent fluid node mean temperature T_m.

Location		Temperature [°F]		ΔT	% Difference
#	r [in]	Tm	Ts	(Ts-Tm)	
1	0.447	264.13	317.26	53.13	18%
2	0.473	275.80	338.00	62.21	20%
3	0.531	291.64	352.95	61.31	19%
4	0.565	309.71	367.36	57.65	17%
5	0.603	333.88	395.54	61.66	17%
6	0.641	358.25	409.50	51.25	13%
7	0.680	385.43	438.13	52.70	13%
8	0.717	417.47	467.26	49.79	11%
9	0.759	456.08	505.93	49.85	10%
10	0.797	511.65	609.01	97.36	17%

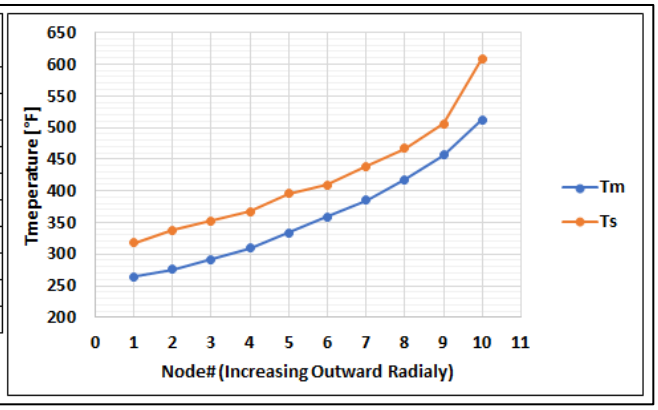

Figure 12. SS max HPT back face temperatures fluid vs. surface (no recirculation flow)

Location		Temperature [°F]		ΔT	% Difference
#	r [in]	Tm	Ts	(Ts-Tm)	
1	0.447	356.97	404.52	47.55	12%
2	0.473	365.76	425.02	59.26	15%
3	0.531	376.96	441.55	64.58	16%
4	0.565	390.00	445.68	55.68	13%
5	0.603	406.20	467.81	61.62	14%
6	0.641	423.64	481.56	57.92	13%
7	0.680	442.81	502.03	59.22	13%
8	0.717	464.87	513.47	48.60	10%
9	0.759	491.45	551.93	60.47	12%
10	0.797	529.53	623.58	94.05	16%

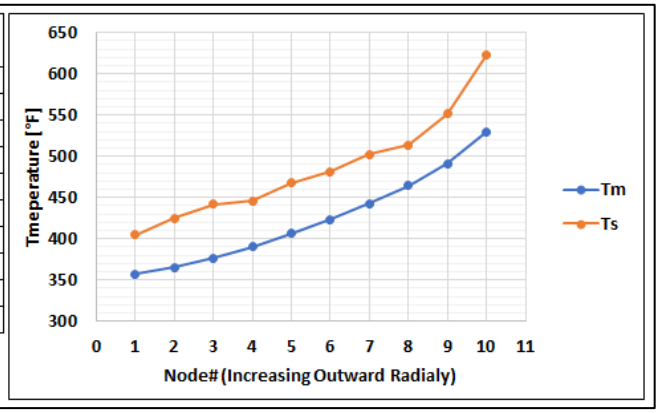

Figure 13. SS max HPT back face temperatures fluid vs. surface (with recirculation flow)

Figures 14-15 are before and after equivalent stress plots of the HPT at the YZ plane. Two peak stresses caused by the thermal gradient occur in the HPT. The first peak stress is located at the back face of the HPT and is the slightly higher of the two. The primary stress component is tensile in the radial direction and is caused by the radial thermal growth of the HPT blades against the cold back face of the HPT. The second stress is located in the fillet at the leading edge of the HPT blades. The stress is primarily tensile in the axial (Z) direction and is also caused by the thermal growth of the blades. This stress is of less concern because the very low volume of material will likely yield and redistribute the stress. On the other hand, the stress on the back face is of concern due to the fatigue life of the material. The implementation of the recirculation loop reduced the peak equivalent stress by 15.5 ksi. This large reduction improved the fatigue life of the HPT to an acceptable level.

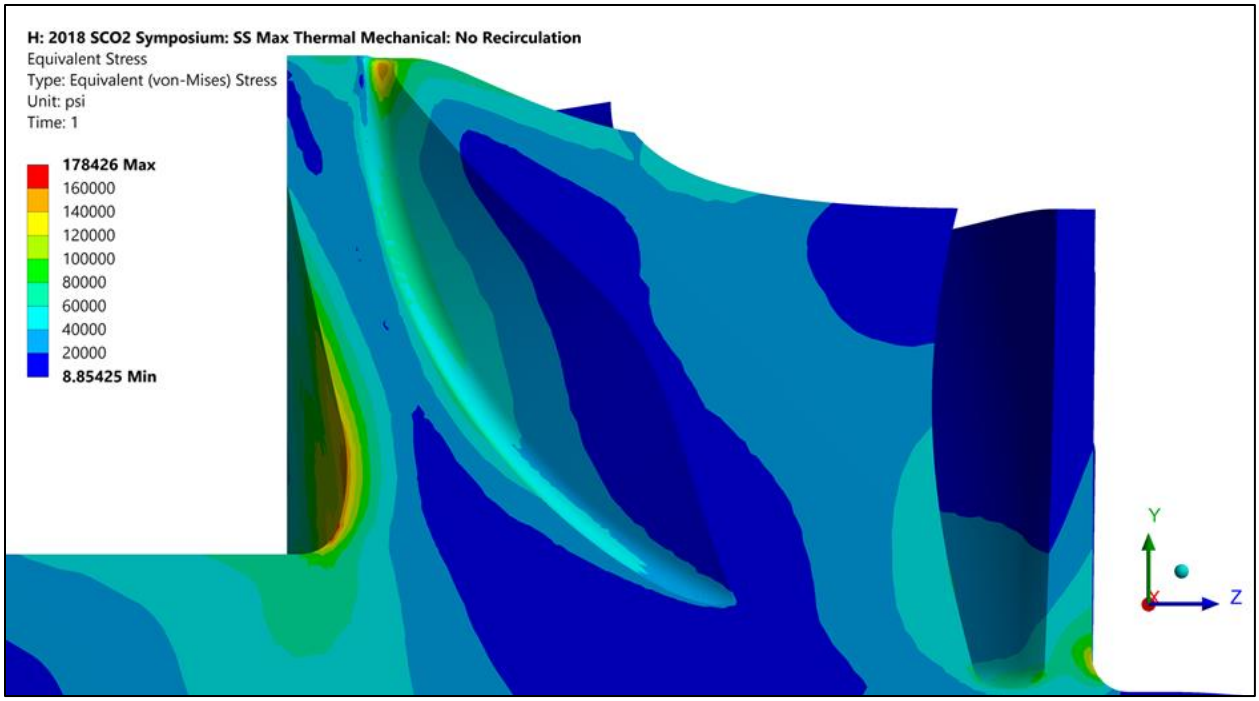

Figure 14. SS max HPT equivalent stress plot (no recirculation flow)

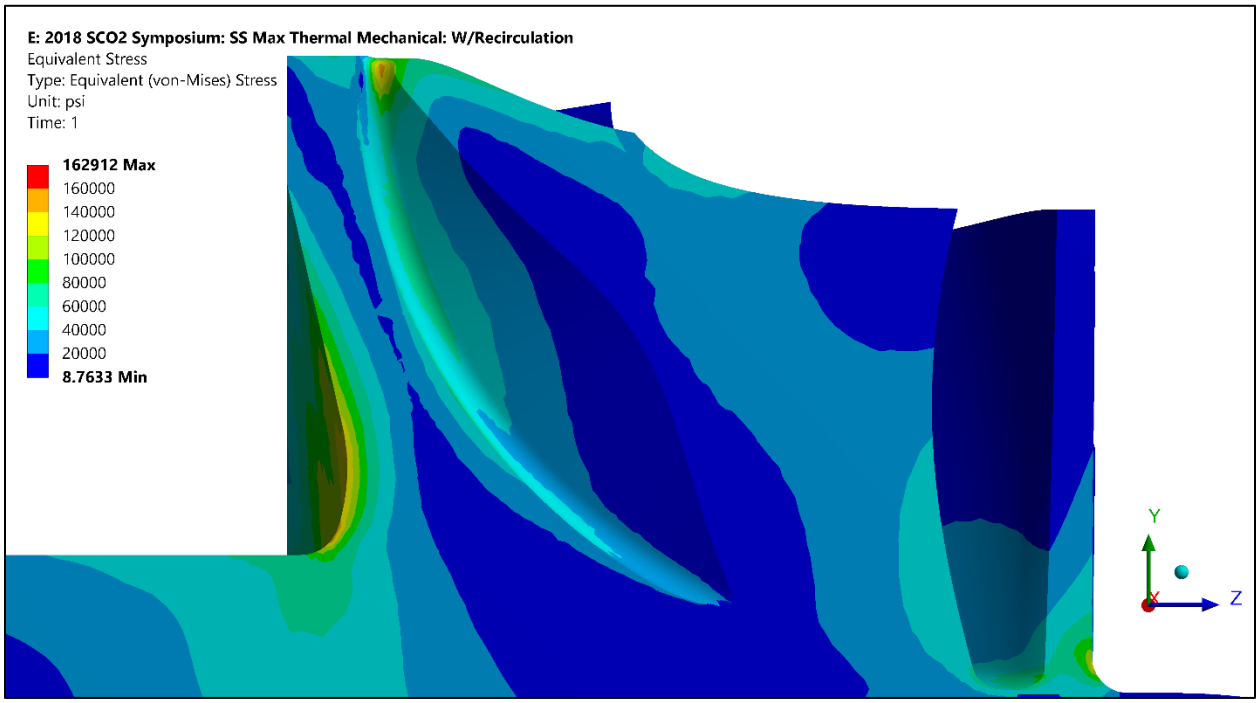

Figure 15. SS max HPT equivalent stress plot (with recirculation flow)

Conclusion

A problem and solution to high thermally induced stresses beyond acceptable fatigue design criteria on the Peregrine 1MW HPT was presented. The problem and solution were contrary to traditional air cooled radial turbine wheels. The root of the problem was high thermal gradients caused by high convective heat transfer on the primary flow and back face surfaces of the HPT. By examining and discussing how sCO_2 and air perform very differently as heat transfer media in turbomachinery the problem was directly linked to the unique thermo-physical properties of sCO_2. This was accomplished via basic heat transfer dimensionless quantities and equations. The examination revealed Nusselt numbers in typical sCO_2 turbomachinery can be over 20x greater than in typical air breathing machines. This conclusion was in agreement with Nusselt numbers calculated in the Peregrine 1MW turbo pump FEA thermal model. Once the root of the problem was identified and better understood a unique and successful secondary flow solution comprised of a preheating recirculation loop was described. An overview of the thermal and structural FEA models utilized to identify and solve the problem was provided. Lastly, thermal and structural model results before and after implementation of the preheating recirculation loop were presented and discussed to show how the stresses were reduced to acceptable fatigue design criteria. Future work may include detailed transient studies on the latency of the preheating recirculation loop.

References

CoolProp. (2016). CoolProp Software.

Yunus Cengel, A. G. (2014). *Heat and Mass Transfer.* McGraw-Hill Higher Education.